Development of Temperature-Stable Thick-Film Dielectrics: III. Role of Glass on the Microstructure Evolution of a Thick-Film Dielectric

Bi-Shiou Chiou, K. C. Liu, Jenq-Gong Duh, and M. C. Chung

Abstract—Glass phase plays an important role in the characteristics of thick-film microelectronics. A dielectric system in $BaTiO_3$ and $SrTiO_3$ containing PbO, B_2O_3, SiO_2, and Al_2O_3 glass constituents is investigated. Microstructure evolution and phase distribution after thermal aging are studied with the aid of electron microscope and X-ray diffractometer. It is observed that the phases in 40 vol% $BaTiO_3$–25 vol% $SrTiO_3$–35 vol% glass thick-film dielectric are not altered after 500°C aging for 480 h. The variation in surface morphology after long time aging is attributed to the precipitation of heavy metal component from the glass which acts as a diffusion species and then dissolves the crystalline phase during firing. The presence of glass in the dielectric enhances the formation of solid solution $(Ba_xSr_{1-x})TiO_3$ and results in the broadening of the Curie peak.

I. INTRODUCTION

GLASS is an important constituent of all thick-film components. Thick-film resistors contain from 60 to 98% glass depending on the sheet resistance. Thick-film capacitors should have a sufficient amount of glass so as to form a continuous vitreous phase, and frit-bonded conductives may be composed of 10% or more glass. During the firing of the thick-film component, glass frits spread and flow to rearrange the microstructure of the component to obtain the desired properties and mechanical integrity [1].

Thick-film components are nonequilibrium systems that depend on a variety of complex physical and chemical processes which proceed to some degree of completion during high temperature processing and are then frozen in when the component is cooled. Some of the processes may restart when the component is employed at a temperature higher than normal applications (i.e., below 125°C), and the drive toward equilibrium may produce irreversible changes in electrical properties. In previous studies, two temperature-stable thick-film dielectrics were developed for high temperature

microelectronics [2]–[6]. One of them is a medium $K(k \sim 100)$ dielectric with composition 40 vol% $BaTiO_3$–25 vol% $SrTiO_3$–35 vol% glass (29 mol% PbO–36.5 mol% B_2O_3–20.4 mol% SiO_2–13.7 mol% Al_2O_3). The presence of the glass phase in this system is to assure complete densification of the dielectric, and the presence of $BaTiO_3$ and $SrTiO_3$ are to give the desired dielectric behavior through temperature-compensation of the dielectrics. However, the aging experiment data indicate that there is a change in dielectric properties during the initial stage, i.e., between 0 and 356 h, of 500°C storage, while no appreciable change is observed afterwards, i.e., between 356 and 1893 h at 500°C. Besides, the crystalline phase is found to dissolve into glass during firing [6]. It is believed that the glass plays an important role in the microstructure evolution of the dielectric during 500°C aging. Hence, the purpose of this research is to study the effect of glass in the dielectric system. Microstructure evolution and phases distribution after 500°C aging are investigated and the interfacial stability between the dielectric and the substrate is evaluated. In addition, impedance spectroscopy is employed to study the electrical behavior of the dielectric.

II. EXPERIMENTAL PROCEDURE

Mixed powders of 40 vol% $BaTiO_3$,[1] 25 vol% $SrTiO_3$,[2] and glass frit [5] were milled for 12 h with Al_2O_3 balls. The slurry was passed through a 325-mesh sieve, and dried with an IR lamp. The dielectric paste was made from the mixed powder blended with 40 vol% screening agent consisting of 10% N-300 ethyl cellulose in butyl carbitol solvent for 2 h in a roll mill.

The capacitor configuration employed is described previously [2]–[4]. The Dupont 4119 chemical bonded gold paste was used as the bottom electrode, printed on an alumina substrate[3] through a 325-mesh screen, dried at 150°C and 350°C, respectively, for 15 min, and then fired at 1020°C for 8 min. Dielectric formulation was printed through a
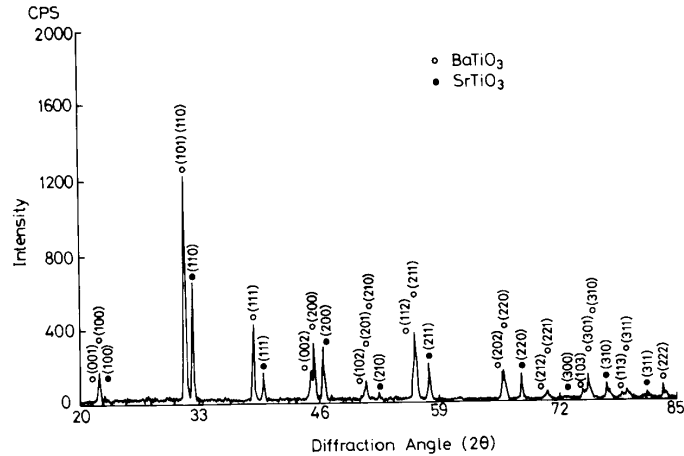
Fig. 1. X-ray diffraction pattern of dielectric paste 40 vol% $BaTiO_3$–25 vol% $SrTiO_3$–35 vol% glass.

200-mesh stainless steel screen, allowed to level at room temperature, dried at 150°C for 15 min to remove the solvent and at 400°C for 15 min to remove the ethyl cellulose, and fired at 800°C for 15 min. Several layers of dielectric were printed and dried in the same manner, while the drying time was elongated to 40 min and it was then fired at 1000°C for 15 min. The thickness of the fired dielectric was about 150–170 μm.

Several specimens without top electrodes were heated with the same firing history as those with top electrode to evaluate the microstructure and elemental distribution. The processes for those with top electrode included drying at 150° and 350°C, respectively, for 15 min, firing at 700°C for 10 min, then furnace cooling. Other specimens for X-ray diffraction were prepared with the same method but with Pt foil as substrate in order to prevent the overlapping problem in diffraction peaks between Al_2O_3 and $BaTiO_3$ or $SrTiO_3$.

Specimens were aged in a 500 ± 10°C oven for periods of aging time. The morphology, elemental distribution, and phases were evaluated with SEM, EPMA, and XRD to probe the influence of aging on the materials system.

III. Results and Discussion

Fig. 1 is the X-ray diffraction pattern of the unfired dielectric paste. There exists $BaTiO_3$ and $SrTiO_3$ as the crystalline phases. The glass frit is amorphous, which makes the background spectrum higher at low diffraction angle, as indicated in Fig. 1. Fig. 2 shows the X-ray diffraction pattern for dielectrics after different aging time at 500°C. The as-fired and aged samples possess a major phase which is a solid solution of $BaTiO_3$ and $SrTiO_3$ with a cubic perovskite structure of lattice constant 3.95 Å. The other phases are $SrTiO_3$ and residual $BaTiO_3$. It appears that there is no phase change for longer periods of aging.

The dielectric firing condition at 1000°C for 15 min and the subsequent thermal aging is not sufficient to assure the equilibrium state of the $BaTiO_3$–$SrTiO_3$ solid solution. Instead of a definite compositions of $BaTiO_3$–$SrTiO_3$ solid
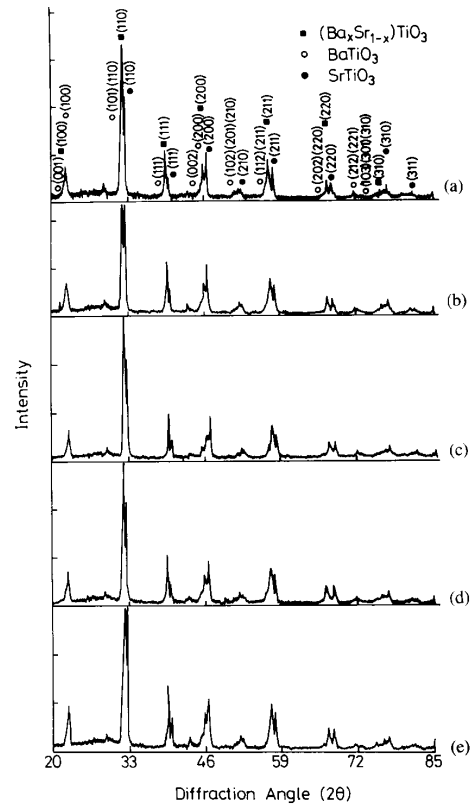

Fig. 2. X-ray diffraction pattern of the fired dielectric film after different aging times. (a) Unaged. (b) 120 h. (c) 264 h. (d) 430 h. (e) 480 h.

solution, continuous compositions of solid solution are formed, i.e., pure $BaTiO_3$, $SrTiO_3$, and compound with intermediate compositions $(Ba_xSr_{1-x})TiO_3$ with $0 \le x \le 1$ are formed, as indicated in Fig. 2. This results in a distribution of Curie temperatures. This can explain the flattening
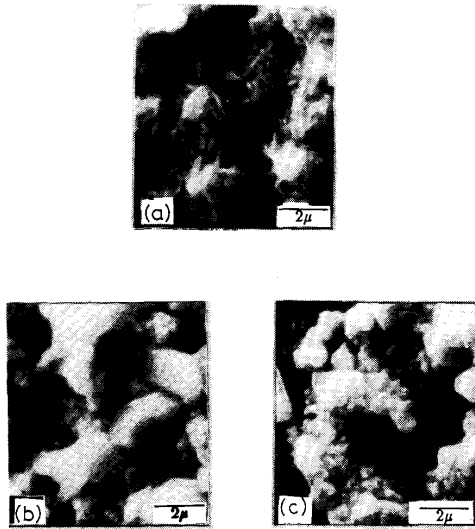
Fig. 3. SEM micrograph of the dielectric film surface with three different structures. (a) Needle-like structures. (b) Sphere. (c) Polyhedron. Sample aged at 500°C for 120 h.
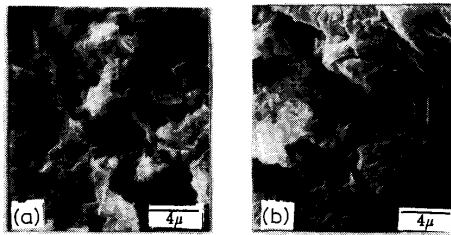

Fig. 4. SEM micrograph of fractured dielectric film without aging. (a) Needle-like and polyhedron structure at inner porous region. (b) Sphere on glass cleavage surface.
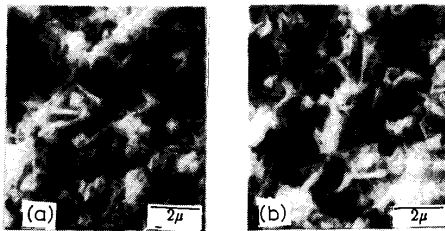

Fig. 5. SEM micrograph of dielectric-film surface including the entangled needle-like structure and ambiguous polyhedron and sphere. Sample aged at 500°C for 285 h.

and broadening of the Curie Peak reported in previous work [6].

The surface morphology of the specimen on alumina substrate is rather complicated. There are three types of structures observed, as illustrated in Fig. 3. They are 1) the needle-like structure on the outer surface, 2) the sphere particle underlying the surface, and 3) the polyhedron extruding from the surface. At the inner porosity of the fractured
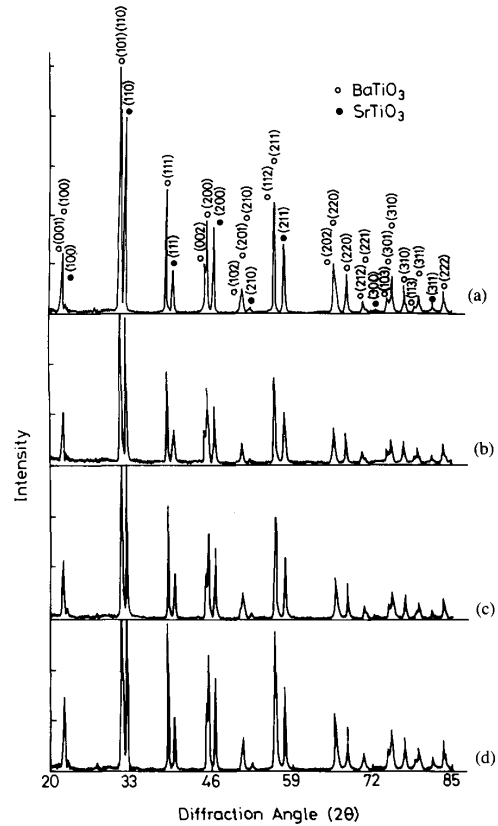

Fig. 6. X-ray diffraction pattern of the fired fritless dielectric film after different aging times at 500°C. (a) Unaged. (b) 120 h. (c) 264 h. (d) 408 h.

dielectric film, the first and the third type structures could be found, while the second one is only observed on the glass cleavage surface, as indicated in Fig. 4. A preliminary study on the $SrTiO_3$-glass system suggested that 0.47 unit volume of $SrTiO_3$ dissolves in one unit volume glass after 15 min at 1000°C. It was reported that as the firing time was increased, some of $SrTiO_3$ precipitated until an equilibrium solubility of 0.22 unit volume was reached [6]. The amount of crystalline phase in this dielectric, i.e., 40 vol% $BaTiO_3$-25 vol% $SrTiO_3$-35 vol% glass, is well above the solubility limit of the glass. Hence, precipitation of $BaTiO_3$ and $SrTiO_3$ occurs during firing and subsequent thermal aging. The needle-like structure, a crystallization phenomenon in thick film, is associated with the heavy metal crystallite precipitation from the glass constituents on surface as described in the work by Hankey *et al.* [7]. The surface is full of the needle-like structure after 285-h aging, while the other structures become less distinctive, as displayed in Fig. 5. A further X-ray mapping analysis reveals that all the elements are uniformly distributed throughout the sample.

The paste containing the $BaTiO_3$ and $SrTiO_3$, but without glass frit, was also fabricated and investigated with the same approach as the one with glass frit to elucidate the contribution of the frit. Fig. 6 shows the X-ray diffraction pattern of
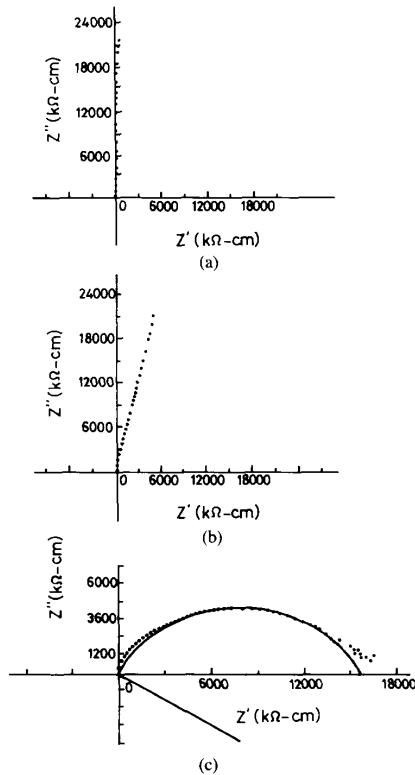
Fig. 7. Complex impedance of the as-fired dielectric 40 vol% $BaTiO_3$-25 vol% $SrTiO_3$-35 vol% glass. Impedance measured at (a) 30°C; (b) 350°C; (c) 500°C.

Fig. 8. Complex impedance of dielectric 40 vol% $BaTiO_3$-25 vol% $SrTiO_3$-35 vol% glass aged at 500°C for 430 h. Impedance measured at (a) 350°C; (b) 500°C.

the paste without glass. Distinct phases of $BaTiO_3$, a tetragonal perovskite structure with $a_0 = 3.993$ Å, $c_0 = 4.024$ Å and $SrTiO_3$, a cubic perovskite with $a_0 = 3.905$ Å are observed. This implies that there exists no solid solution reaction for dielectric without glass after firing and 500°C aging.

The glass frit is employed in the so-called liquid phase sintering to enhance the solid solution reaction. It acts as a diffusion media and tends to dissolve the original crystalline phases during firing. The firing process is usually short and is finished well before the solid solution reaction is complete. The dissolved constituents result in precipitation during aging, and render the surface morphology vary as shown above, which represents the prominent alteration in the morphology development of the dielectric film during the aging process.

The electrical behavior of the thick-film dielectric is studied with the aid of an impedance analyzer.[4] Figs. 7-9 are the complex impedance plots of the as-fired, 430-h aged, and 600-h aged sample, respectively. The impedance plot for an ideal dielectric is shown schematically in Fig. 10. The semicircle at the higher frequency range represents the lattice (bulk) behavior inside the grain, while the other semicircle at
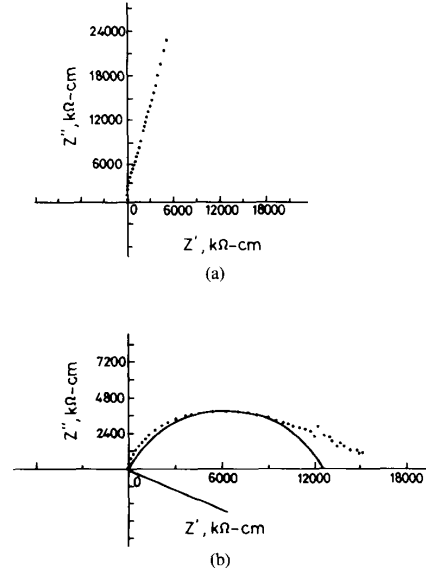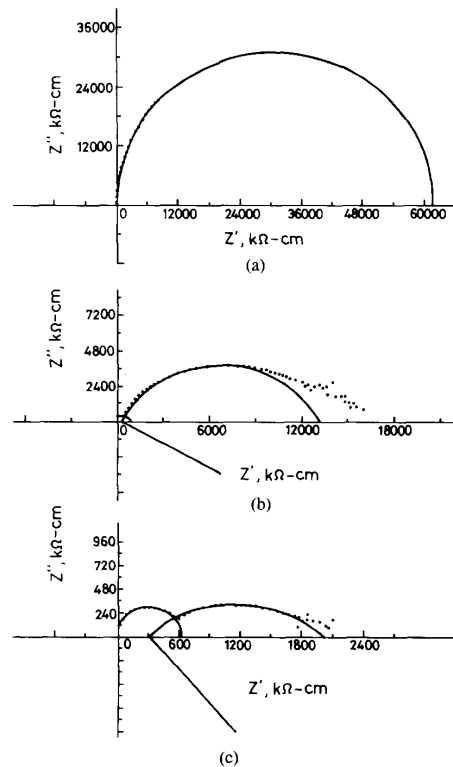
Fig. 9. Complex impedance of dielectric 40 vol% $BaTiO_3$-25 vol% $SrTiO_3$-35 vol% glass aged at 500°C for 600 h. Impedance measured at (a) 30°C; (b) 500°C; (c) 608°C.

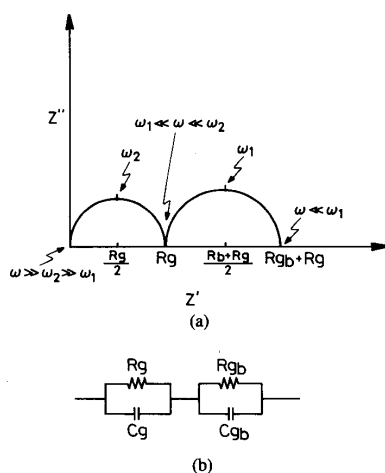[4] HP 4192 A, Yokogawa-Hewlett-Packard, Tokyo, Japan.

Fig. 10. (a) Impedance plot and (b) equivalent circuit model of an ideal
dielectric.

the lower frequency range indicates the grain boundary char-
acteristics [8]. As shown in Figs. 7-10, it is found that the
as-fired dielectric is very "capacitive" at room temperature
(Fig. 7(a)). The dielectric loss increases at higher tempera-
ture and after thermal aging for longer time (Figs. 7(b)-9).
However, a non-Debye dielectric behavior is observed for
samples measured at 500°C and higher temperature (Figs.
7(c), 8(b), 9(b), and (c)). This means that both the permittiv-
ity and dielectric loss are frequency dependent, which is
consistent with the polarization phenomenon in $BaTiO_3$ ce-
ramics [9]. It is argued that the increase in dielectric loss
after thermal aging is related to the heavy metal component
precipitation from the glass as mentioned previously. How-
ever, the detail is subject to further investigation. In fact, the
grain boundary characteristic of sample after thermal aging
becomes prominent as the semicircle at the lower frequency
range shows up as indicated in Figs. 7-9. It should be
pointed out that the microstructure of the thick-film dielectric
is fairly complicated and detailed investigation is needed to

reveal the correlation between the microstructure and the
electrical behavior of the dielectric.

IV. Conclusions

1) The phase of thick-film dielectric 40 vol% $BaTiO_3$-25
   vol% $SrTiO_3$-35 vol% glass is not altered after 500°C
   aging up to 480 h.
2) Glass in the dielectric enhances the formation of solid
   solution $(Ba_xSr_{1-x})TiO_3$, which is related to the flat-
   tening and broadening of the Curie peak.
3) The surface of the dielectric is filled with the needle-like
   structure after 285 h aging at 500°C. The needle-like
   structure, resulting from crystallization, causes an in-
   crease in the dielectric loss.

Acknowledgement

References

[1] R. W. Vest, "Conduction mechanisms in thick film microcircuits,"
    Final Tech. Rep. on Contracts DAHC-15-70-G7 and DAHC-15-73-
    G8, Dec. 1975.
[2] B. S. Chiou and R. W. Vest, "High temperature thick film di-
    electrics," *Bull. Amer. Ceram. Soc.*, vol. 63, no. 6, pp. 811-815,
    1984.
[3] B. S. Chiou, "Development of temperature-stable thick-film di-
    electrics: I. Low K dielectric," *IEEE Trans. Comp. Hybrids
    Manuf. Technol.*, vol. 12, pp. 789-797, 1989.
[4] ——, "Development of temperature-stable thick-film dielectrics: II.
    Medium-K dielectric," *IEEE Trans. Comp. Hybrids Manuf.
    Technol.*, vol. 12, pp. 798-808, 1989.
[5] B. S. Chiou and R. W. Vest, "Glasses for high temperature thick-film
    systems," *Bull. Amer. Ceram. Soc.*, vol. 63, no. 6, pp. 816-820,
    1984.
[6] B. S. Chiou, "High temperature thick film dielectrics," Ph.D. disser-
    tation, Purdue Univ., W. Lafayette, IN, 1981.
[7] D. L. Hankey, J. A. Goldman, and P. J. Moran, "Structure property
    relationships in experimental thick-film interfaces," *Solid State
    Tech.*, vol. 27, no. 9, pp. 268-273, 1984.
[8] B. S. Chiou, H. T. Dai, and J. G. Duh, "Electrical behavior of
    Ceria-stabilized Zirconia with rare-earth oxide additives," *J. Amer.
    Ceram. Soc.*, vol. 73, no. 4, pp. 866-871, 1990.
[9] B. S. Chiou, S. T. Lin, J. G. Duh, and P. H. Chang, "Equivalent
    circuit model in grain-boundary barrier layer capacitors," *J. Amer.
    Ceram. Soc.*, vol. 72, no. 10, pp. 1967-1975, 1989.